Chapter 2

Investigations of MIMO Antenna for Smart Mobile Handsets and Their User Proximity

Hari Shankar Singh

Additional information is available at the end of the chapter

http://dx.doi.org/10.5772/intechopen.75002

Abstract

In this chapter, a monopole antenna with compact size, simple structure, easy to fabricate is reported which covers LTE700 (band13/14) (746–798 MHz), GSM1800 (1710–1885 MHz), PCS1900 (1850–1990 MHz), and LTE2600 (2500–2690 MHz) band based on 6-dB return loss. The proposed MIMO antenna consists of two radiating elements. The main radiating element is a composition of driven element, which is directly fed with microstrip line, and one parasitic element. The parasitic element provides the resonance at higher frequency band and the combination of driven elements and parasitic elements provide above-said frequency bands. The current distribution, far-field radiation patterns, and diversity parameters are checked out for the MIMO antenna in free space. Further performances are studied in the presence of user proximity.

Keywords: diversity antenna, planar antenna, mobile phone, user proximity

1. Introduction

The fourth generation and Wi-MAX technologies require high data rates and longer range so that the end users can enjoy the quality service. In order to accomplish this, wireless communication systems have to be pushed to the physical limits of the radio channels [1]. As "a key to gigabit wireless" multiple-input multiple-output (MIMO) technology as a diversity

scheme made a great breakthrough for raising the performance with high-speed transmission rates, high-quality mobile communication services without the need of any additional frequency spectrum or power [2, 3]. The vast potential of MIMO techniques is manifested by rapid espousal into the wireless standards, such as LTE (Long Term Evolution), UMTS, and Wi-MAX [4–7].

LTE standard is used for high speed and better quality communication of mobile phones and data terminals that can integrate MIMO technologies for reducing fading phenomenon, increasing channel capacity, and could be incorporated into handheld mobile applications [8, 9]. The most challenging task in MIMO systems is to enforce multiple antennas on handheld terminals as small as mobile handsets. Now-a-days, the slimness of mobile phone has been tremendously increased therefore, to keeping the volume of an antenna small, became a difficult task. The antennas are required to be small, designed with in the small volume and yet their functioning has to be maintained to achieve high gain, wide bandwidth, and low correlation coefficient. The use of inductors and capacitors are, to match of the resonance frequency, tuning of the frequency bands, and to increase the electrical length, but simultaneously reduces the bandwidth and the efficiency of the antenna due to these chip elements. Some of the literature available to make antenna electrically small size, and to obtain wider impedance bandwidth [10, 11]. A dual electrically small MIMO antenna system for 4G terminals was presented by Sharawi et al. which covered the band of 760–886 MHz [10]. Zhang et al. presented a wideband LTE MIMO antenna in mobile handset operating at 740 MHz [11]. The matching level and central frequency are tuned by the shunt capacitor of the port and the series inductor. Shen et al. introduce a wideband diversity antenna which operates in a very wide bandwidth of 1200 MHz starting from 1700 to 2900 MHz [12]. A compact Tri-band MIMO/diversity antenna for mobile was proposed which covers LTE band (765–787 MHz), PCS 1900 (1850–1920 MHz) and Wi-Max (3050–3650 MHz) [13]. The above-proposed antennas are complex in terms of fabrication (loaded with chip components like inductors and capacitors) and in design.

2. Antenna design and configuration

Figure 1(a) illustrates the specific geometry of the proposed antenna, consisting of two symmetrical back to back monopole antenna elements, which are printed on the upper corners of the mobile circuit board (FR4 substrate with $\varepsilon r = 4.4$ and $\tan \delta = 0.02$). The two antenna elements are considered in this study which are placed near to the corner of mobile phone. The dimension of the substrate is chosen as $120 \times 60 \times 0.8$ mm^3. On the upper surface of the substrate, the main rectangular ground of dimension 104×60 mm^2 is disposed. The volume of the single antenna element is $16 \times 21 \times 7$ mm^3 which are mounted at the top corner of the mobile circuit board. The enlarged view of the single unfolded antenna element is given **Figure 1(b)** whereas **Figure 1(c)** shows the detailed dimensions of the proposed slot configuration on the ground plane. Detailed dimensions of the unfolded metal strip are shown in **Figure 1(d)**. All optimized parameters are shown in **Table 1**.

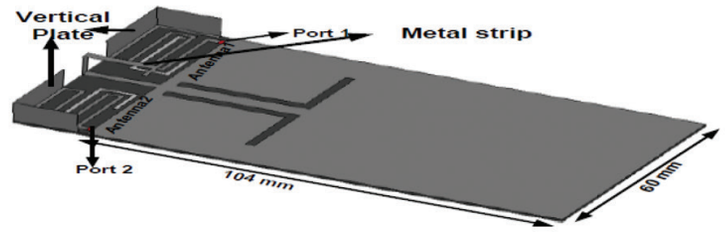

(a)

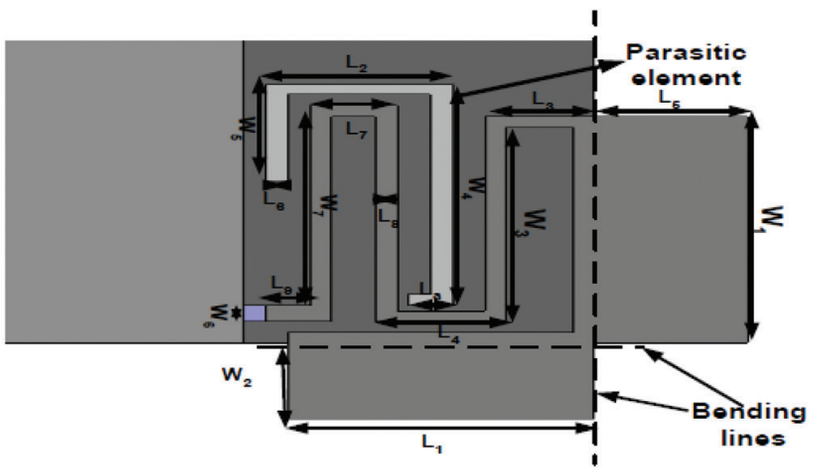

(b)

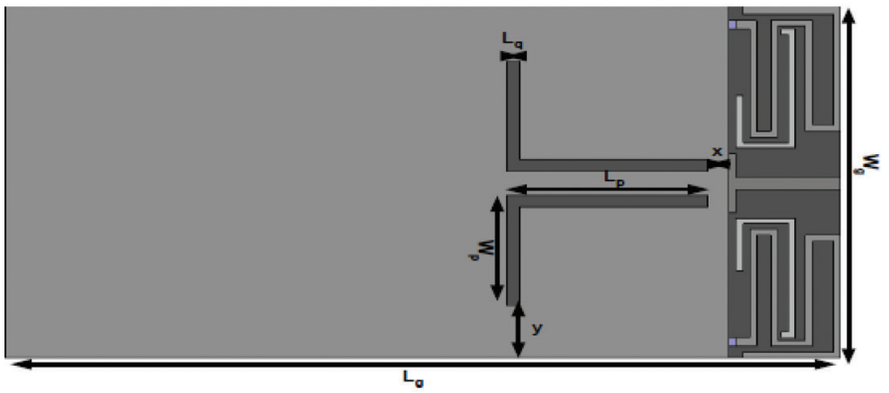

(c)

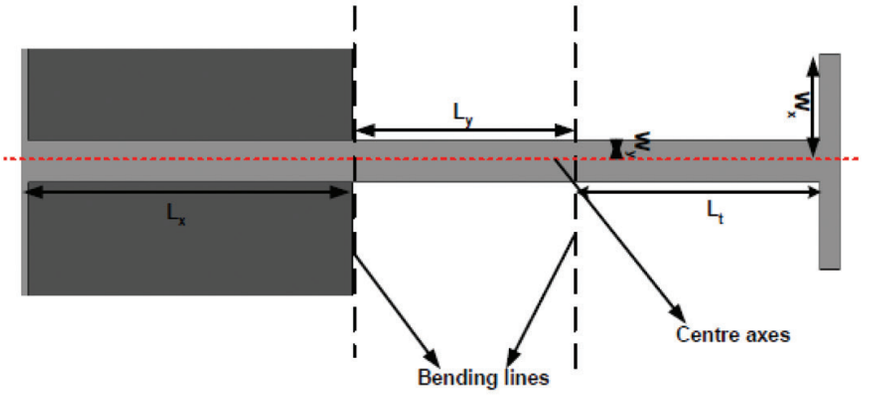

(d)

Figure 1. (a) Configuration of the proposed antenna (b) detail dimensions of the unfolded proposed antenna (c) detail dimensions of the slot cut on the ground (d) detail dimensions of the unfolded metal strip inserted between the antennas.

Parameter	Value (mm)	Parameter	Value (mm)	Parameter	Value (mm)
L_g	120	L_6	1	W_6	1.5
W_g	60	L_7	4	W_7	18.5
L_1	14	L_8	1	L_a	10
W_1	21	L_9	2	L_q	2
L_2	8.5	W_2	7	L_p	27
L_3	5	W_3	18	W_p	17
L_4	6	W_4	20.5	x	3
L_5	7	W_5	9	y	9
L_x	16	L_y	7	L_t	16
W_x	5	W_y	1		

Table 1. Optimized shape parameters of the proposed antenna.

3. Results and discussions

3.1. *S*-parameter analysis

All the simulations are carried out on finite element method (FEM) based high-frequency structure simulator (HFSS). **Figure 2** shows the optimized *S*11 and *S*21 parameters of the proposed antenna. The reported antenna covers operating band at lower frequency side from 736 to 822 MHz, and at higher frequency side from 1609 to 2057 MHz, and from 2491 to 2785 MHz based on the 6-dB return loss. Which covers the LTE700 (band13/14), GSM1800, PCS1900, and LTE2600 mobile communication bands. The achieve isolation between MIMO

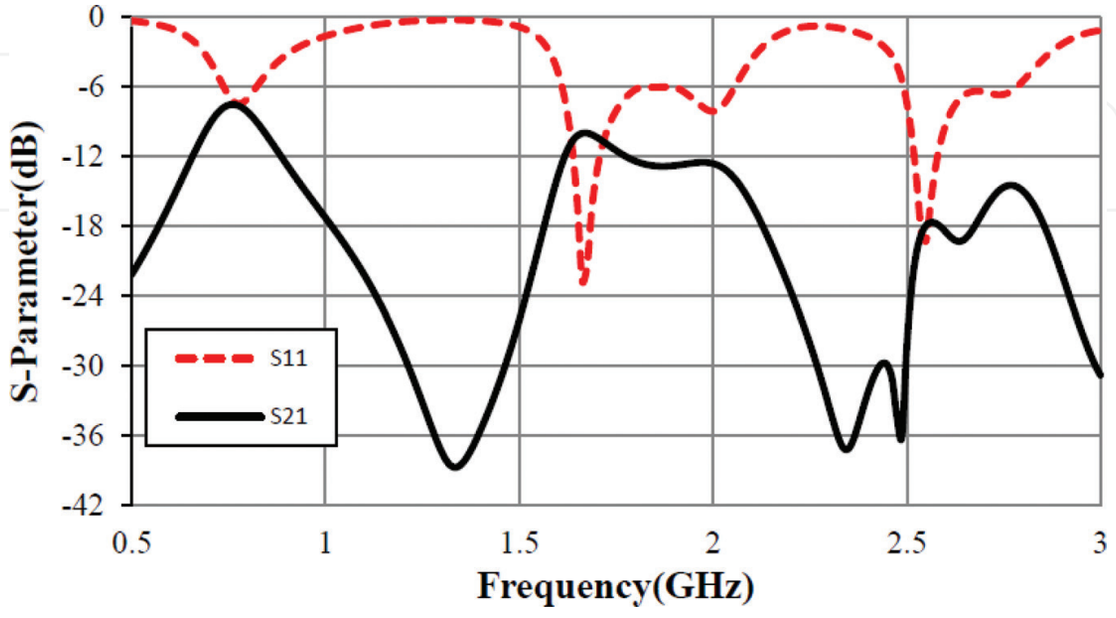

Figure 2. *S*-parameter of the proposed MIMO antenna.

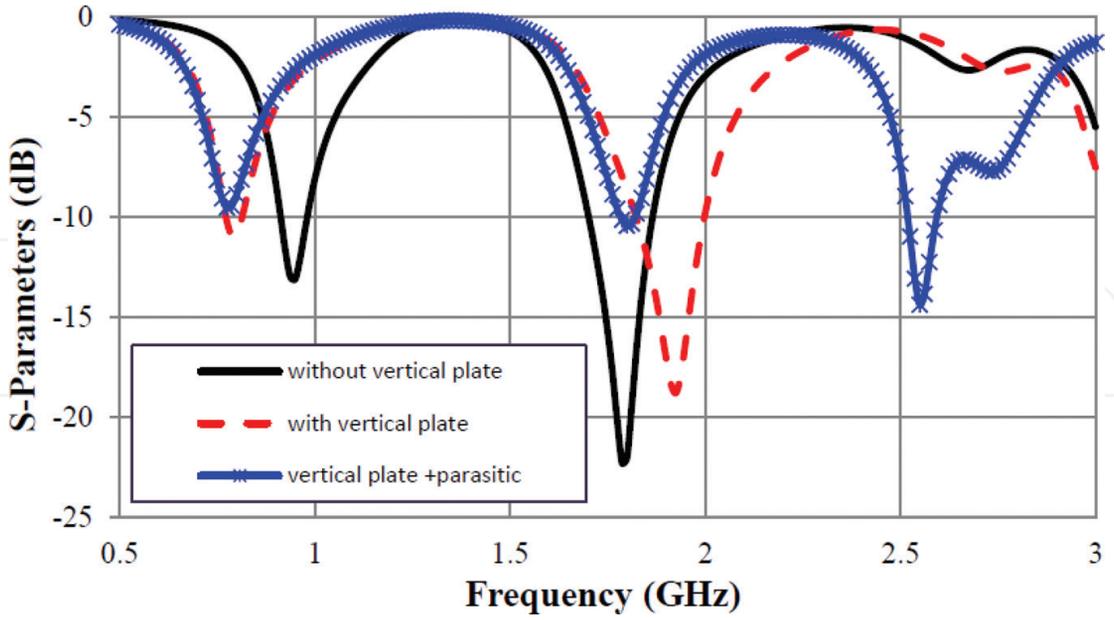

Figure 3. Effect of the vertical plate and the parasitic element on the *S*-parameters.

antenna elements are −7.5 dB across 775 MHz (736–822 MHz), −10 dB across 1660 MHz (1609–2057 MHz), and better than −18 dB over 2.55 GHz (2491–2785 MHz).

The main driven element which is directly fed by a microstrip line is designed to resonate at 937 MHz simultaneously higher modes provide another resonance centered at 1787 MHz. A parasitic element is used which resonates at 2.55 GHz. To achieve the LTE700 frequency band the vertical plate is added to the main radiating element due to which the electrical length is increased correspondingly the lower operating frequency is shifted from 937 to 762 MHz as shown in **Figure 3**.

3.2. Parametric analysis

Figure 4 shows the variation of *S*-parameters with different configurations. There are two different configurations analyze to see the effect on *S*-parameters. In the first configuration, only ground slot is present means no metal strip present between antenna elements, due to this modification the isolation is increased at higher frequency side whereas the isolation remains same at lower frequency side. When the only metal strip is present means no ground slot the bandwidth enhancement is observed. Further, these two modifications combined into single structure and variation of *S*-parameters is shown in **Figure 5**. It is observed that isolation, as well as bandwidth, gets enhanced by adding metal strip and slot on the ground.

Some key parameters are optimized for proper bandwidth and impedance matching at lower frequency side as well as higher frequency side. **Figure 6** shows the effect of 'W_1' on *S*-parameters. It is seen that as 'W_1' increase, bandwidth decreases at the middle band and bandwidth increases at the upper frequency whereas isolation over operating bands almost unaffected. The optimized value for 'W_1' is 21 mm. **Figure 7** shows the effect of the parameter 'W_x'. It is observed that as the value of 'W_x' increases, the isolation at 1.65 GHz, and at 2.54 GHz decreases. The optimized value of 'W_x' is 5 mm.

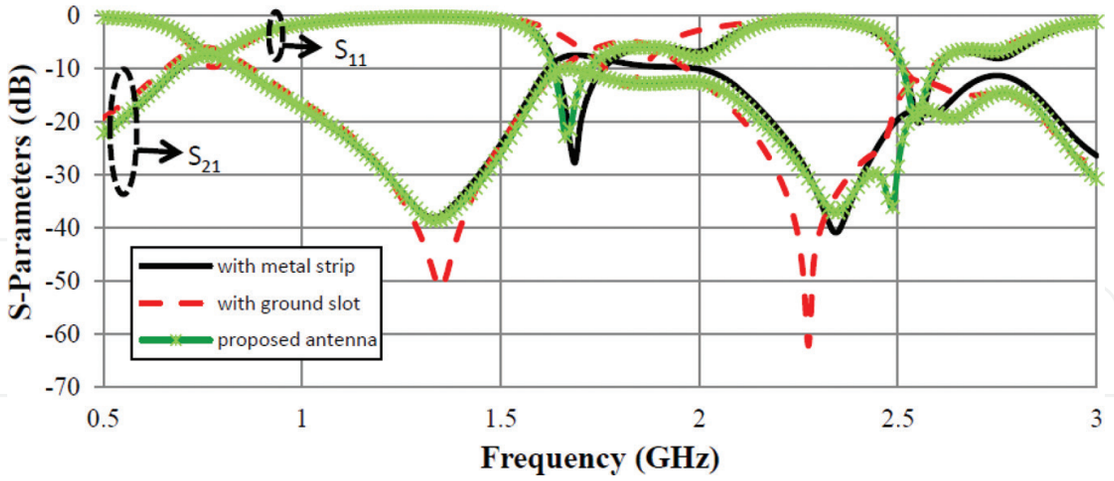

Figure 4. Individual effects of the ground slot and metal strip on *S*-parameter.

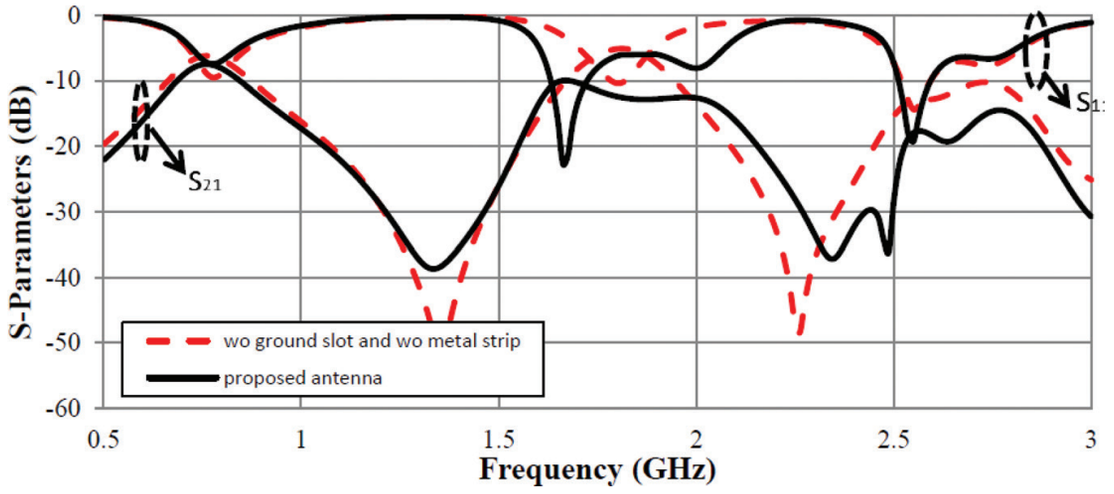

Figure 5. *S*-parameters of the proposed antenna without any isolation techniques and with both the techniques.

3.3. Surface current distribution

Figure 8 shows surface current distributions are shown at 775, 1660, 1810, and 2545 MHz when antenna 1 is excited and antenna 2 is matched terminated. These figures validate the role of slot structure and the metal strip as it is clearly observed that most of the current is present nearby the excited antenna and is trapped in and around the slot structure, thus preventing the flow of current into the second antenna. In this way, the two antennas are less coupled to each other which are the basic requirement of MIMO antenna array.

3.4. 3D far field radiation patterns

The CST MWS is used to plot the 3D far field radiation patterns. The 3D far-field radiation patterns are shown in **Figure 9**. In the case of MIMO antenna system, only one port is excited while keeping other port matched terminated with the 50 Ω load. The radiation patterns

http://dx.doi.org/10.5772/intechopen.75002

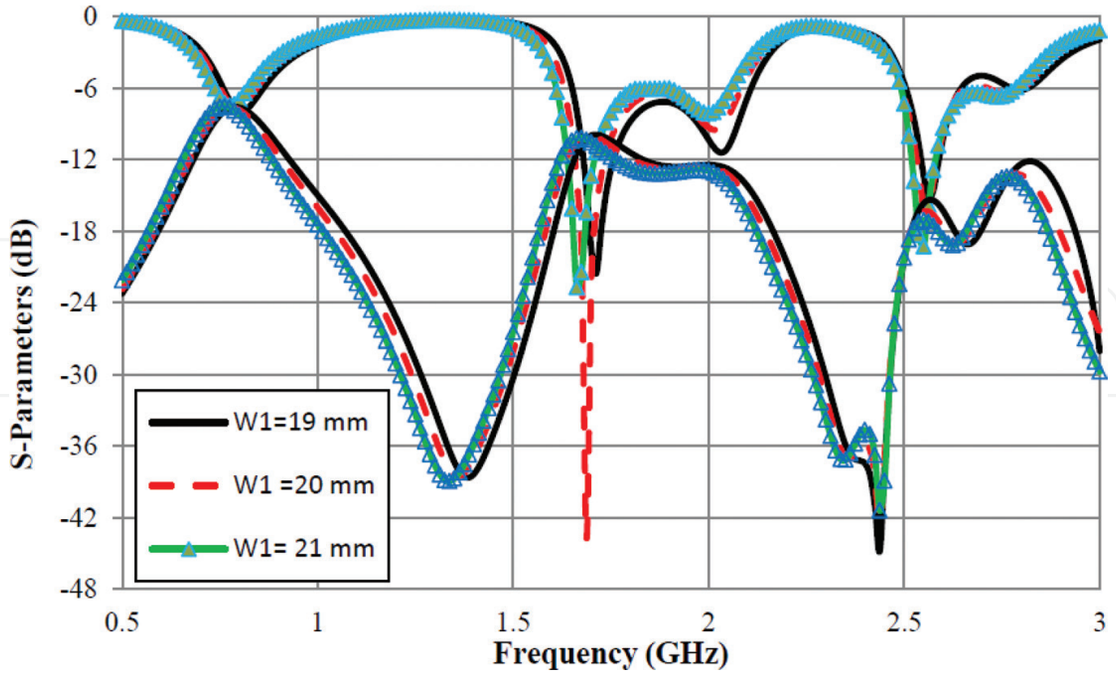

Figure 6. Effect of length 'W_1' on the *S*-parameters.

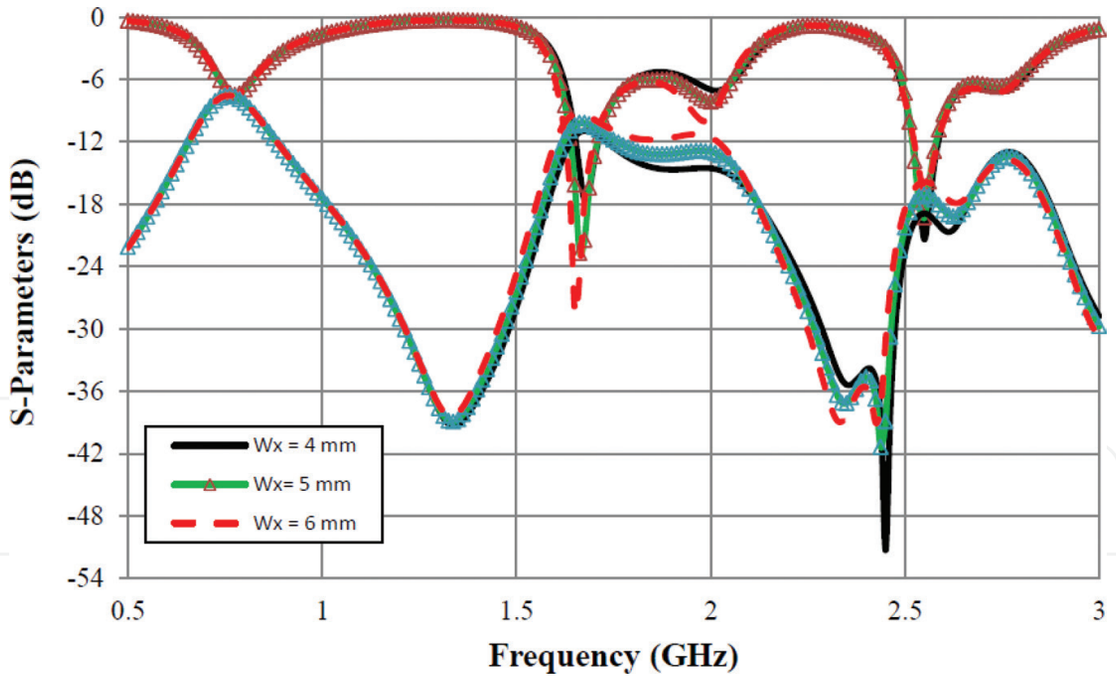

Figure 7. Effect of length 'W_x' on the *S*-parameters.

of Antenna 1 and Antenna 2 are almost mirror images of each other over all the operating frequency bands. That means they are covering the complementary space regions and indicating that the proposed MIMO antenna has good pattern diversity characteristics.

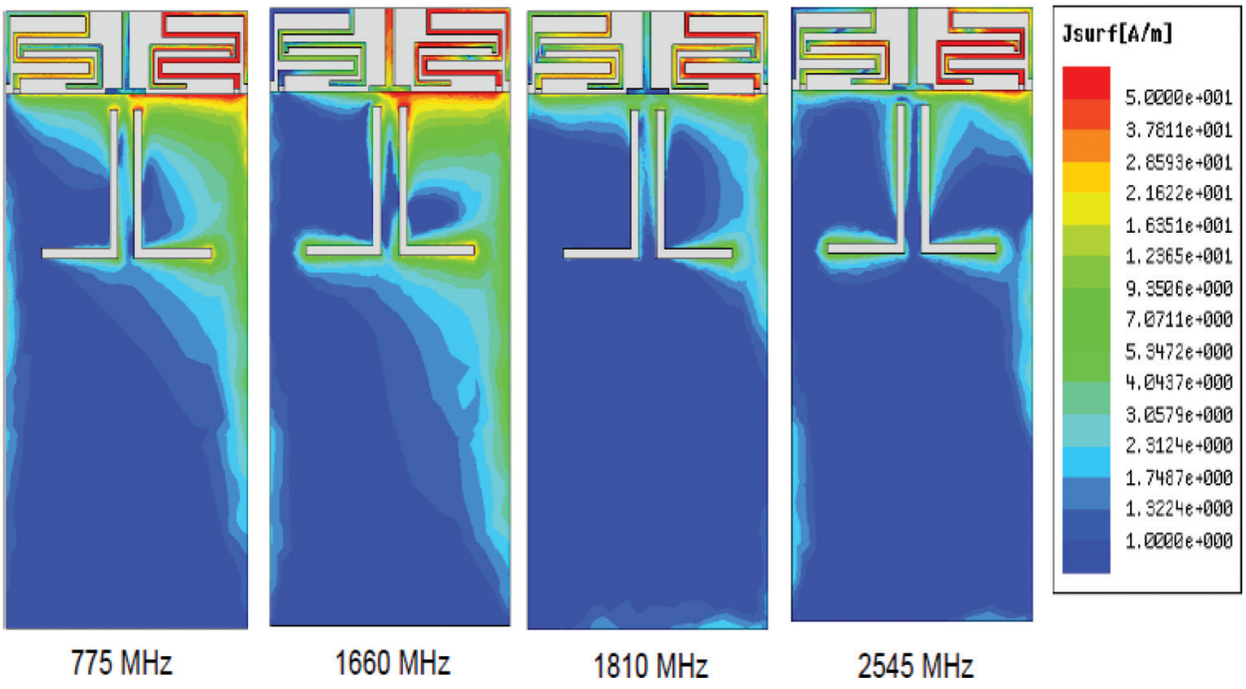

Figure 8. Surface current distributions when the Antenna1 is excited and antenna 2 is matched.

3.5. Diversity characteristics of the proposed antenna

The diversity performance of the proposed MIMO antenna is evaluated by the MEG, correlation coefficient, and diversity gain.

3.5.1. Mean effective gain (MEG)

The MEG values determined MIMO antenna system and given in **Table 2**. The values for MEG1 and MEG2 are almost identical (less than 3 dB difference) and the ratio of MEG1 with MEG2 is close to 1 which satisfies the equality criterion for the two antennas. **Figure 10** shows the computed MEG for Antenna 1 when assuming mv = mH = 0° and σv = σH = 20°. It is observed that the computed MEG decreases with increasing the frequency.

3.5.2. Envelope correlation coefficient (ECC)

To evaluate the performance of the proposed MIMO antenna, key performance parameter is ECC. **Figure 11** shows the simulated ECC for the proposed MIMO antenna. The ECC is obtained well below 0.25 for all the operation bands which are practically acceptable.

3.5.3. Diversity gain (DG)

The effectiveness of diversity is given in terms of diversity gain. Diversity gain is calculated using equation (1):

$$DG = \left[\frac{\gamma_c}{\Gamma_c} - \frac{\gamma_1}{\Gamma_1}\right]_{p(\gamma_c \le \gamma_g/\Gamma)} \quad (1)$$

http://dx.doi.org/10.5772/intechopen.75002

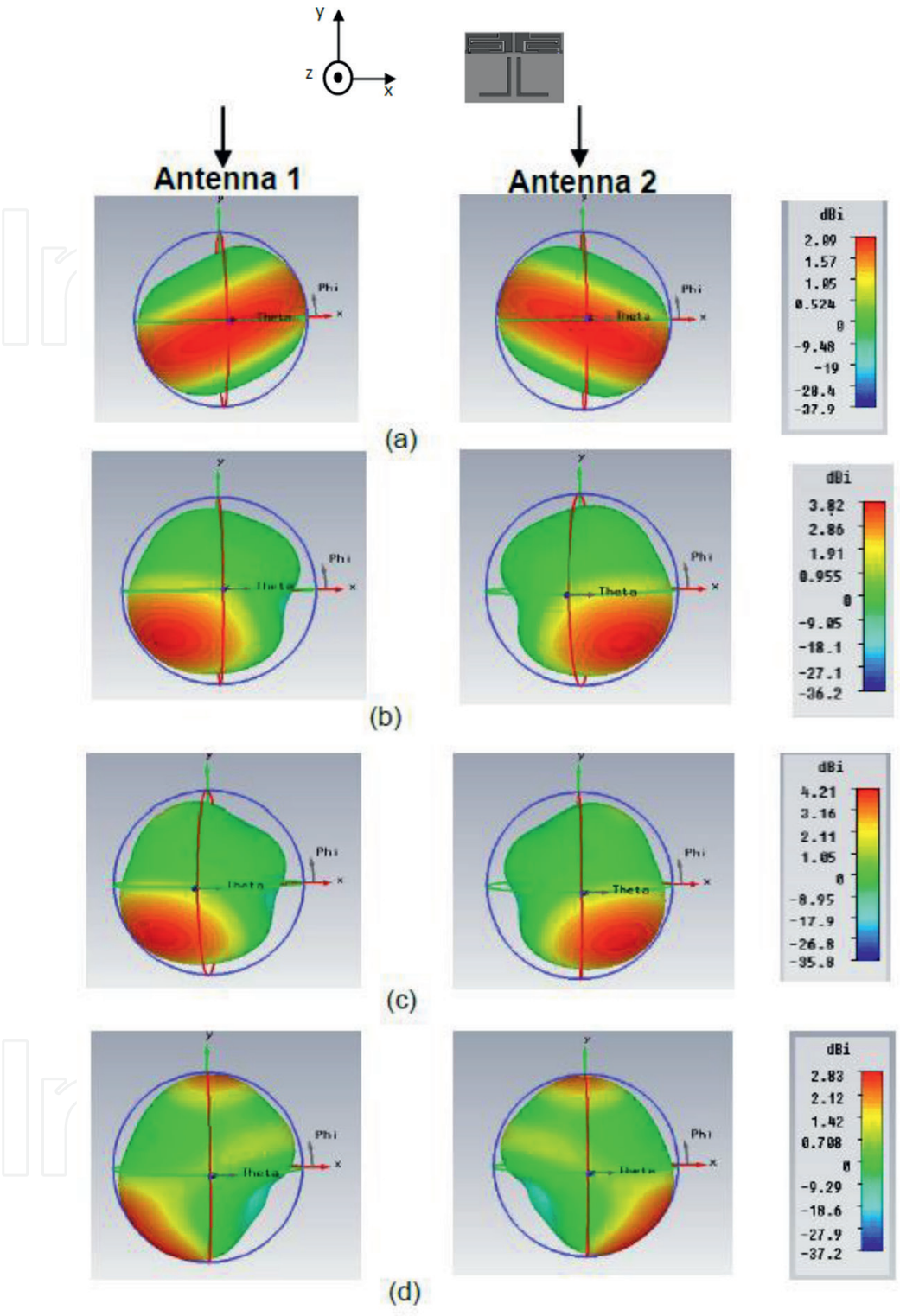

Figure 9. 3D far field radiation patterns at different frequencies (a) 775 MHz, (b) 1660 MHz, (c) 1810 MHz, and (d) 2545 MHz.

where, γ_c is the instantaneous SNR of the diversity combined signal, Γ_c is the mean SNR of the combined signal, γ_1 is the highest SNR of the diversity branch signals, Γ_1 is the mean value of γ_1, and γ_s/Γ is a threshold or reference level.

Mean effective gain	Frequency (GHz)		
	0.77	**1.66**	**2.54**
MEG1	−4.3533	−4.8742	−6.0447
MEG2	−4.3625	−4.8624	−6.0210
MEG1/MEG2	0.9978	1.0024	1.0039

Table 2. MEG at different frequencies.

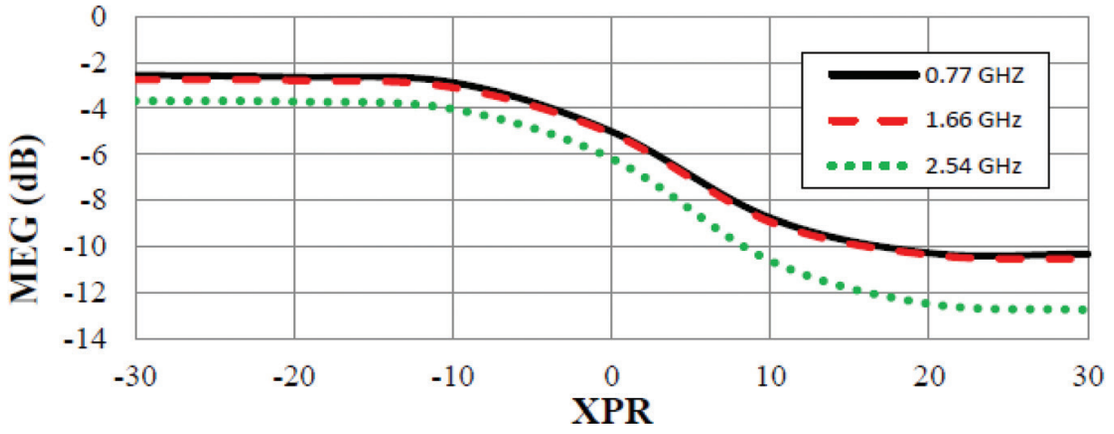

Figure 10. Variation of MEG of antenna 1 with XPR computed.

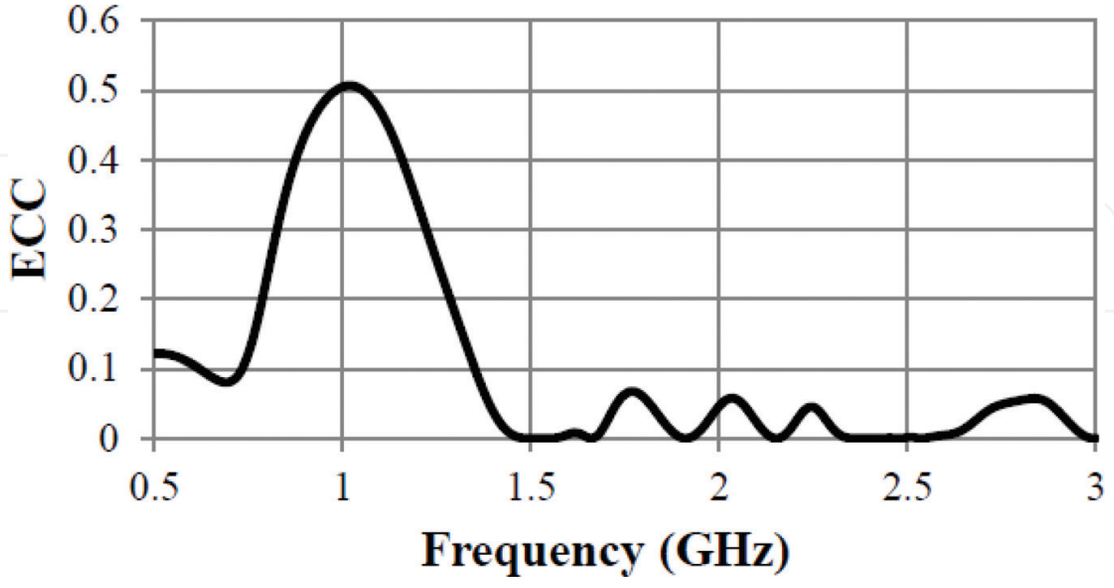

Figure 11. Variation of ECC with frequency.

4. User proximity analysis

4.1. Simulations set-up

The effect of mobile phone configuration (all the major metallic components) is studied for the proposed antenna by keeping the mobile phone antenna at top of the mobile circuit board in talk mode (SAM head and hand). Further, three commonly user style is considered to analyze the user's proximity. **Figure 12(a)** shows talk mode which includes SAM head and PDA hand. Further, to study the data mode (PDA hand) and read mode (dual hand) in addition to the talk mode, the simulation set-up is created in computer simulation technology microwave studio (CST MWS) [14]. **Figure 12(a)** shows two layers head tissue model (fluid and cells) and antenna along with mobile phone configuration (LCD, battery, buttons, speaker, camera, microphones, connectors, and housing) in Talk mode. **Figure 12(b)** shows the hand tissue model and antenna locations for the Data mode. The hand model and holding rules are exactly the same as in the Talk mode, the only difference is that there is no human head model in Data mode. **Figure 12(c)** shows read mode. The user's body *"SAM head and PDA hand (Talk mode)"; "PDA hand (Data mode)" + and position of the mobile phone (antenna with the mobile environment) are in accordance with the cellular telecommunication industry association (CTIA) [15]. Generally, there are three commonly used ways in which users' use their mobile phone i.e. Talk mode, Data mode, and Read mode. In the simulations, human head consists of two layers namely, fluid and cells whereas fluid is confined within the cells and hand model consists of only one layer. The dielectric properties of the human tissue are used in this study can be found in [15]. However, the placement of multi-antenna systems over mobile circuit board is symmetrical with respect to the other mobile circuitry. Hence, any hand of the user (left or right will not cause any difference. In the simulations, we have

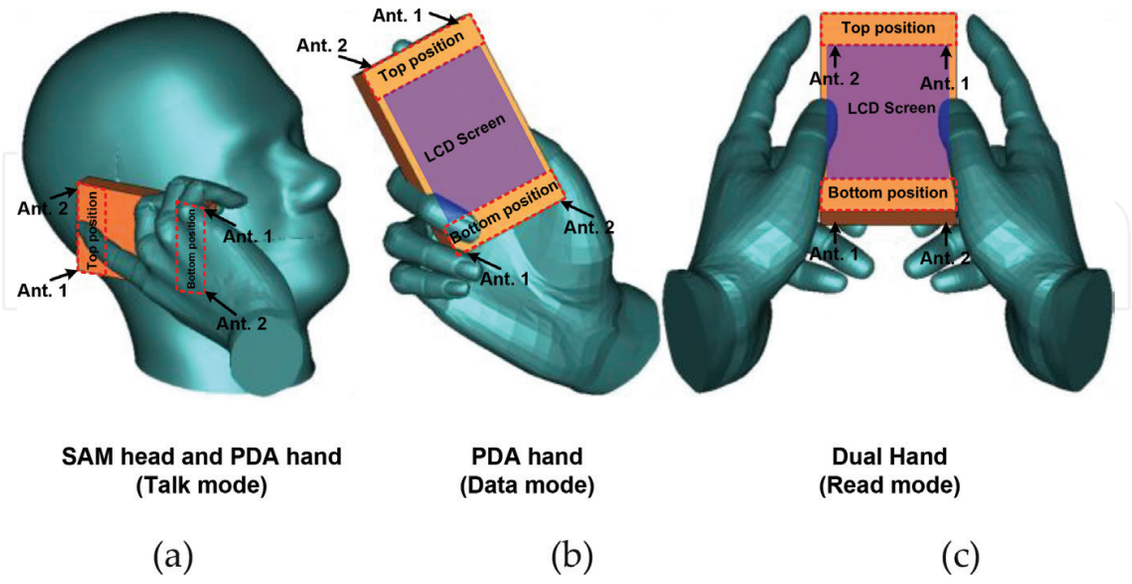

Figure 12. User proximity (a) SAM head and PDA hand, (b) PDA hand, and (c) dual hand.

considered right hand to hold the mobile phone (as most people do). Further, the position of the antenna over mobile circuit board is considered at top and bottom for each case of user proximity. The antenna placed near to the human ear is considered as top position while near to the human mouth is considered as a bottom position of the antenna.

4.2. Channel capacity loss (CCL)

The next important parameters channel capacity loss (CCL) employed to characterize equality of a multi-antenna array. Thus, the CCL is also investigated in free space and user proximity for top and bottom position antenna array. It is computed using *S*-parameter [16] and formula is given as;

$$C_{loss} = -\log_2 \det(\psi_R) \tag{2}$$

where, ψ_R is the receiving antenna correlation matrix. The matrix elements ϱij stands the correlation. The expression shows MIMO systems performance and Closs affect by the reflections at the antenna ports.

$$\psi_R = \begin{pmatrix} \rho_{11} & \rho_{12} \\ \rho_{21} & \rho_{22} \end{pmatrix} \tag{3}$$

here,

$$\rho_{ii} = 1 - \left|S_{ii}\right|^2 - \left|S_{ij}\right|^2 \tag{4}$$

$$\rho_{ij} = -\left(S^* ii^* S\, ij + S^* ji^* S\, ij\right) \quad \text{for i, j = 1 or 2}$$

The calculated values of CCL for the multi-antenna array in free space and user proximity are given in **Table 3**. In the free space, the measured CCL is in close agreement with simulated one. Moreover, calculated CCL in user proximity provides high value for the bottom-placed antenna in comparison to the top placed antenna array this is due to high correlation between multi-antenna arrays. For the good MIMO antenna performance, CCL should be less than 0.4 bits/s/Hz. From the **Table 3**, it is depicted that the values are well below 0.4 bits/s/Hz in free space as well as in user proximity.

4.3. Specific absorption rate (SAR) analysis

The effect of radiation from the antenna in human tissues can be evaluated by specific absorption rate (SAR) [15]. The Cellular Telecommunication Industry Association (CTIA) standard is used to calculate the SAR of multi-antenna systems and simulation setup is shown in **Figure 13**. The American standard federal communication commission (FCC) postulate 1.6 W/kg average 1 g tissues, while the European standard postulate 2 W/kg average over 10 g tissues. The stimulating power for SAR calculation is 24 dBm at a lower frequency (0.777 GHz) and 21 dBm for higher frequency (1.9, 2.1, and 2.5 GHz). The calculated values of SAR are given in **Table 4**. As

Frequency (GHz)/Users condition			Antenna at top	Antenna at bottom
0.777	Free space	Simulated	0.37	0.29
		Measured	0.35	0.35
	Talk mode		0.38	0.28
	Data mode		0.3	0.25
	Read mode		0.28	0.2
1.9	Free space	Simulated	0.27	0.21
		Measured	0.21	0.25
	Talk mode		0.24	0.29
	Data mode		0.2	0.19
	Read mode		0.28	0.19
2.1	Free space	Simulated	0.29	0.21
		Measured	0.21	0.29
	Talk mode		0.14	0.13
	Data mode		0.12	0.12
	Read mode		0.14	0.12
2.5	Free space	Simulated	0.2	0.21
		Measured	0.24	0.21
	Talk mode		0.19	0.15
	Data mode		0.17	0.17
	Read mode		0.14	0.18

Table 3. Variation of CCL in free space and user proximity.

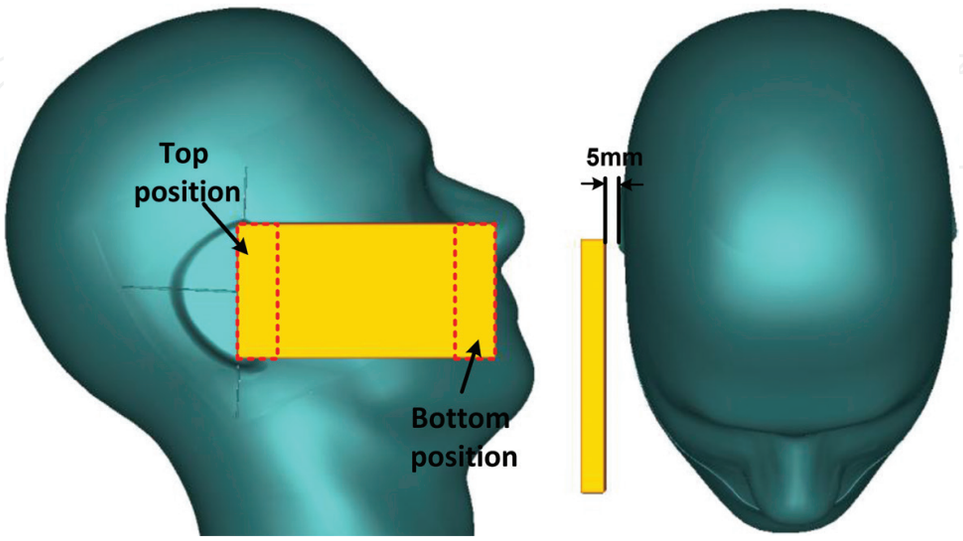

Figure 13. SAR setup according to CTIA.

Antenna	Freq.	0.777 GHz	1.9 GHz	2.1 GHz	2.5 GHz
		Top position			
Ant. 1 (W/kg)	FCC	0.6	0.7	0.78	0.49
	European	0.29	0.31	0.43	0.21
Ant. 2 (W/kg)	FCC	0.7	1.2	0.95	0.68
	European	0.42	0.37	0.64	0.29
		Bottom position			
Ant. 1 (W/kg)	FCC	0.38	0.39	0.24	0.33
	European	0.38	0.29	0.28	0.15
Ant. 2 (W/kg)	FCC	0.42	0.38	0.37	0.24
	European	0.3	0.29	0.27	0.21

Table 4. SAR values for the head phantom.

per the simulation setup, the distance between head phantom and the bottom-placed antenna is more, result in lower SAR while top located antenna provides larger SAR values. It is interestingly noted that lower SAR values are achieved for both standards because of the plastic box cover the mobile phone antenna. It can also be observed that SAR values of Ant. 1 and Ant. 2 is slightly different for top and bottom placed elements due to non-planar phantom. The calculated values of SAR follow the defined standard.

5. Conclusion

In this chapter, a quad-band monopole MIMO antenna covering LTE13/14, GSM1800, PCS1900, and LTE2600 is presented. The proposed antenna consists of an antenna and parasitic plate which resonates at 762, 1787, and 2550 MHz with good return loss. By introducing the vertical plate shifting of lower frequency from 937 to 762 MHz is observed. Enhancement of bandwidth and isolation is observed by cutting slot on the ground and by placing the metal strip in between the antennas. With these features, as well as compact and simple configuration, the proposed MIMO antenna is appropriate for the mobile handsets. The study of user proximity confirms that the proposed antenna suitable for mobile handsets.

Author details

Hari Shankar Singh

Address all correspondence to: harishankar1990@gmail.com

Department of Electronics and Communication Engineering, Thapar Institute of Engineering and Technology, Patiala, Punjab, India

References

[1] Chiau CC. Study of the diversity antenna array for the MIMO wireless communication systems. [Ph. D. Thesis] UK: University of London; 2006

[2] Paulraj A, Gore D, Nabar R, Bolcskei H. An overview of MIMO communications–a key to gigabit wireless. Proceedings of the IEEE. 2004;**92**:198-218. DOI: 10.1109/JPROC.2003.821915

[3] Farhadi H, Wang C, Skoglund M. Distributed transceiver design and power control for wireless MIMO interference networks. IEEE Transactions on Wireless Communications. 2014;**14**:1199-1212. DOI: 10.1109/TWC.2014.2365202

[4] Ogawa K, Uwano T. A diversity antenna for very small 800-MHz band portable telephones. IEEE Transactions on Antennas and Propagation. 1994;**42**:1342-1345. DOI: 10.1109/8.318664

[5] Jensen MA, Samii YR. Performance analysis of antennas for hand-held transceivers using FDTD. IEEE Transactions on Antennas and Propagation. 1994;**42**:1106-1113. DOI: 10.1109/8.310002

[6] Singh HS, Meruva B, Pandey GK, Bharti PK, Meshram MK. Low mutual coupling between MIMO antennas by using two folded shorting strips. Progress in Electromagnetics Research B. 2013;**205-221**(2013):53. DOI: 10.2528/PIERB13052305

[7] Vaughan RG, Andersen JB. Antenna diversity in mobile communications. IEEE Transactions on Vehicular Technology. 2013;**VT-36**:149-172. DOI: 10.1109/T-VT.1987.24115

[8] Sesia S, Toufik I, Baker M. LTE-The UMTS Long Term Evolution: From Theory to Practice. Chichester, U.K.: Wiley; 2009. DOI: 10.1002/9780470742891

[9] Wong K, Kang T, Tu M. Internal mobile phone antenna array for LTE/WWAN and LTE MIMO operations. Microwave and Optical Technology Letters. 2011;**53**:156-157. DOI: 10.1002/mop.26038

[10] Sharawi MS, Faouri YS, Iqbal SS. Design and fabrication of a dual electrically small MIMO antenna system for 4G terminals. In: Proceedings of the 6th German Microwave Conference; 14-16 March 2011. Darmstadt, Germany: IEEE; 2011. pp. 1-4

[11] Zhang S, Zhao K, Ying Z, He S. Diagonal antenna-chassis mode and its application for wideband LTE MIMO antennas in mobile handsets. In: Proceeding of International Workshop on Antenna Technology (iWAT); 4-6 March 2013. Sweden: IEEE; 2013. pp. 1-4. DOI: 10.1109/IWAT.2013.6518376

[12] Shen SD, Guo T, Kuang F, Zhang X, Wu K. A novel wideband printed diversity antenna for mobile handsets. In: Proceeding IEEE 75th Vehicular Technology Conference (VTC Spring); 6-9 May 2012. Yokohama: IEEE; 2012. pp. 1-5. DOI: 10.1109/VETECS.2012.6240173

[13] Singh HS, Bharti P, Pandey GK, Meshram MK. A compact tri-band MIMO/diversity antenna for mobile handsets. In: Proceeding IEEE CONECCT; 17-19 January 2013. Bangalore, India: IEEE; 2013. pp. 1-6. DOI: 10.1109/CONECCT.2013.6469306

[14] Computer Simulation Technology Microwave Studio (CST MWS), [Online] available: http://www.cst.com

[15] "Test plan for mobile station over the air performance," CTIA revision 3.1, January 2011

[16] Choukiker YK, Sharma SK, Behera SK. Hybrid fractal shape planar monopole antenna covering multiband wireless communications with MIMO implementation for hand-held mobile devices. IEEE Transactions on Antennas and Propagation. 2014;(3):1483-1488. DOI: 10.1109/TAP.2013.2295213